Explicit time integration methods applied to nonlinear beam model

Oleksandr Hubanov
Vilnius Gediminas Technical University

January 6, 2021

Abstract

Itroduction

Review of an integration schemes for nonlinear forces been done in [1], By investigating the characteristics of both the non-linear elastic and the nonlinear damped Hertzian contact models, it has been found that higher orders of accuracy are recoverable and depends on the degree of the governing non-linear equation. The numerical errors of the linear and nonlinear force models are however markedly different in character.

Symplectic Euler, Forward Euler, Backward Differenced, Runge–Kutta, Adams–Bashforth been compared [2] The recommended solver for any large scale system would be the Symplectic Euler scheme due to its ability to produce near sec- ond order results, its general high accuracy, simple implementation and low storage requirements.

The numerical errors in idealised discrete element method (DEM) simulations are reviewed in [3] The truncation error has a superlinear relationship with the simulation time-step, Δt. Reducing Δt substantially reduces ϵ; however, increasing the number of time-steps required in a simulation inevitably increases the round-off error. This implies that there is an optimal, implementation- specific choice of Δt, which minimises the total error.

Efficacy of contact dynamics (CD) in a variety of indeterminate problems, including some involving multiple materials, non-spherical shapes, and nonlinear contact constitutive laws been shown in [4].

A brief overview is given on the capabilities and on the current limitations of the Discrete Element Method (DEM) coupled with Computational Fluid Mechanics (CFD) to simulate chemical reacting moving granular material.[5]

Impact of particle shape is inspected in [6] Simulations show that sediment particle's shape effect on its motion is more obvious in laminar flows rather than in turbulent flows.

Dynamic stability of beam structures for 8, 16 and 32 layers been investigated at [7]

Among Euler, semi-implicit Euler, Runge-Kutta and Leapfrog, we found that simulation with Leapfrog numerical integration characterizes a mass-spring-damper system best in terms of the energy loss of the overall system. [8]

Modelling approach

Investigating motion of any mechanical system comes to integration motion equation of discrete parts of this system. Chordae tindae presents itself as fibrous tissue and could be described as system of 1D rods, in case of getting mechanical equivalent of system. Example of such flat 2D system are shown on figure 3.

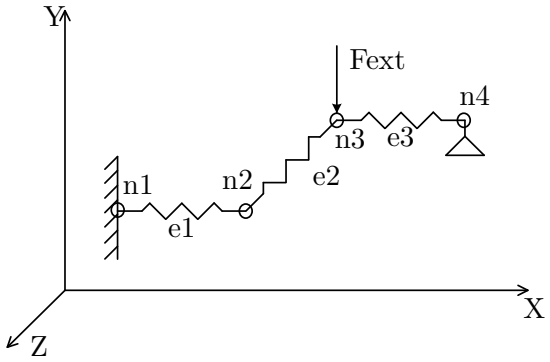

Figure 1: 1D Rod system in global coordinate system

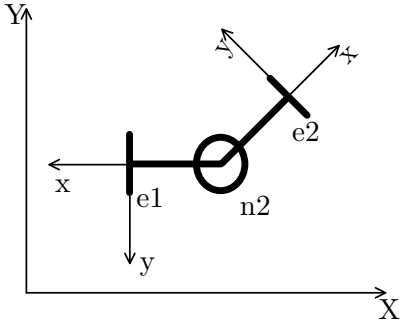

Figure 2: Extracted node from system

Model discribed as series fo soft fibers. Each ec

System consists of discrete elements e_1, e_2 and e_3. All elements are connected to each other through nodes n_2, n_3 and to special points through n_1 and n_4. Each element e_n of system has own orientation in global coordinate system. From schematic representation of node comes that all vector variables of node should be calculated in global coordinate system and element variables in own local coordinate system(figure 3). For transformation between coordinate systems direction cosine matrix (DCM)(1) can be used.

$$DCM = \begin{bmatrix} cos(X,x) & cos(X,y) & cos(X,z) \\ cos(Y,x) & cos(Y,y) & cos(Y,z) \\ cos(Z,x) & cos(Z,y) & cos(Z,z) \end{bmatrix} \quad (1)$$

where $\{X, Y, Z\}$ is global coordinate system and $\{x, y, z\}$ is local coordinate system.

According to primitive scheme of node 3, mass of each node can be calculated, like sum of half mass of each element, which acting in node. $m_n = \sum_e m_e/2$

In case that node does not have external interrupt, like pressure or other applied force, schematic represent of node can be as on figure 3.

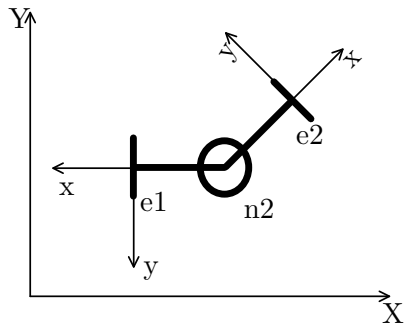

Figure 3: Extracted node from system

Mathematical model of discrete system is expressed by equations of nodes motion. All system acting in global coordinate system $\{X, Y, Z\}$ and each element acting in own local coordinate system $\{x, y, z\}$.

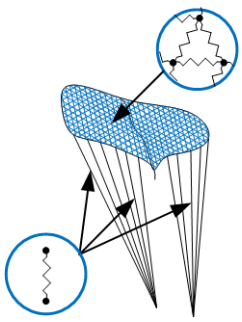

Figure 4: Displacement of papillary muscle over cardiac cycle

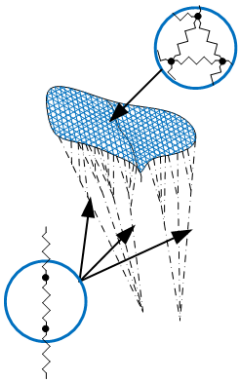

Figure 5: Displacement of papillary muscle over cardiac cycle

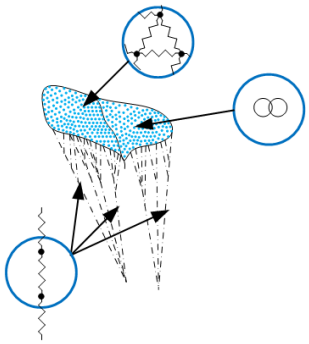

Figure 6: Displacement of papillary muscle over cardiac cycle

research aim is to compare 1 rod and rope of rods

If express kx and $c\dot{x}$ by $\sum F_{elem}$, then motion equantion will become to:

$$\vec{F}_{inertia} = \vec{F}_{ext} - \sum \vec{F}_{elem} \quad (2)$$

F_{ext} is external load force, applied to node in global coordinates. Value of this force for each time step is loaded from list of loads. F_{elem} is sum of internal forces of each element, which acting in node. From each element counts only half of force to node, other half going to neighbour node. For 1D rod system F_{elem} can be expressed like:

$$F_{elem} = \sum_e N_e(x) \quad (3)$$

To words about mechanical properties of valve components, poisson ratio ν is same, 0.49 for all. Mean value of chordae length L $0,025m$ and diameter d $0,001m$. Chordae has density ρ = 1040 kg/m3 and stiffness $E = 2000N/m$, when leaflets has ρ = 1.06E3 kg/m3 and $E = 2MPa$ (Anterior leaflet), $E = 1MPa$ (Posterior leaflet)

Mathematical model

The motion of chordae as motion of physical object can be expressed by Newton's equation of motion:

$$m\vec{\ddot{x}} = \vec{F} \tag{4}$$

where F is internal force of object, m – mass of object and $\ddot{x}$ is acceleration, k – stiffness coefficient of object, x is displacement of object and c – damping coefficient of object, $\dot{x}$ is velosity of object.

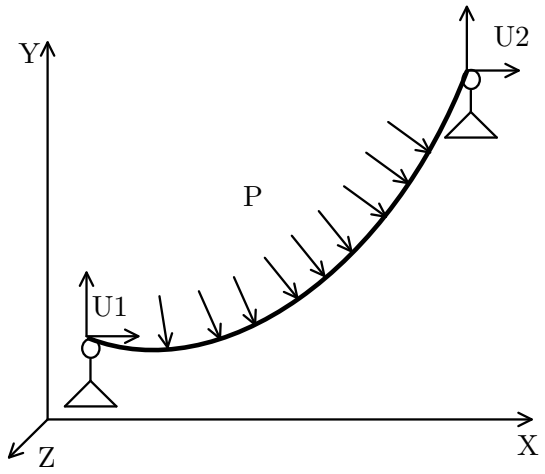

Figure 7: Chordae tindae in global coordinate system

Initial conditions are: $x(0) = 0$ and $\dot{x}(0) = V_0$. Acceleration could be known from (4) as:

$$\vec{\ddot{x}} = \vec{F}/m \tag{5}$$

Than Euler's scheme of integration can be described like:

$$\vec{\dot{x}}(t + \Delta t) = \vec{\dot{x}}(t) + \vec{\ddot{x}}(t)\Delta t \tag{6}$$

$$\vec{x}(t + \Delta t) = \vec{x}(t) + \vec{\dot{x}}(t)\Delta t \tag{7}$$

Linear deformation

Internal object force becomes from physical deformation of object it self. In linear case of study, deformation of element much less compare to element dimensions. It is expressed by linear geometry equation(8), which showing relation between initial length of element and length in Δt state.

$$\varepsilon = \frac{dU}{dx} = \frac{l(\Delta t) - l(t)}{l(t)} \tag{8}$$

According to Hook law $\sigma = \varepsilon E$ and linear geometry equation (8), inner force can be described as:

$$\begin{aligned} N(x) &= \int_{Al} \varepsilon E dl dA = EA \int_{l} \varepsilon dl \\ &= \frac{EA}{l(t)} * (l(t + \Delta t) - l(t)) \end{aligned} \tag{9}$$

where $l(\Delta t)$ is current length of chordae, $l(t)$ length of chordae at previuous time moment, E – Young's modulus for chordae, A – volume of chordae. To be able to integrate equation of motion, need to express deformation in equation (9) by differences between displacements of nodes, to which chordae is connected:

$$N(x) = \frac{EA}{l(t)} * (x_i(t) - x_j(t)) \tag{10}$$

Nonlinear deformation

Nonlinearity in main mean that chordae can get huge deformation compare to its demesions. Equation of F_{elem} in this case would change to nonlinear form:

$$N(x) = \int_t \int_A \sigma dA dt \tag{11}$$

From this equantion comes that cross sectional area and stiffness coefficient will get nonlinearity.

Changing of cross sectional area over time of chordae is changing its length over time. Linear geometry equation(8), showing linear relations between length, because difference in Δt state takes according initial length of chordae. In case of huge deformation need to recalculate length of chordae on each time step and take difference of displacement according to previous time step. In end of geometry equation become to nonlinear form:

$$\varepsilon = \frac{dU}{dx} = \frac{l(\Delta t) - l(t - \Delta t)}{l(\Delta t)} \tag{12}$$

Inner force(9) also become to nonlinear form:

$$\begin{aligned} N(x) &= \int_t \int_A \varepsilon E dA = EA \int_t \varepsilon \\ &= \frac{EA}{l(\Delta t)} * (l(\Delta t) - l(t - \Delta t)) \end{aligned} \tag{13}$$

where l is current length of element, l_0 length of element at $t = 0$, E – Young's modulus for element material.

And nonlinear equantion of inner force for integration:

$$N(x) = \frac{EA}{l_0} * (U_i - U_j) \tag{14}$$

Integration technics

HAVE NO IDEA HOW TO START THIS SECTION

Euler first order explicit

$$\begin{aligned} v(t+\Delta t) &= v(t) + a(t) * \Delta t \\ x(t+\Delta t) &= x(t) + v(t) * \Delta t \end{aligned} \tag{15}$$

The central difference scheme, also known as velocity Verlet is a very widely used integration method of second order. Velocities in the upcoming time step $t + \Delta t/2$ and positions at $t + \Delta t$ are calculated as

$$\begin{aligned} v(t+\Delta t/2) &= v(t+\Delta t/2) + a(t-\Delta t/2) * \Delta t \\ x(t+\Delta t) &= x(t) + v(t+\Delta t/2) * \Delta t \end{aligned} \tag{16}$$

The fourth order Gear's method (GPC4). In the prediction step positions and their higher derivatives are calculated based on Taylor series expansions as

$$\begin{aligned} b(t+\Delta t, p) =& b(t) \\ a(t+\Delta t, p) =& a(t) + b(t) * \Delta t^2 \\ v(t+\Delta t, p) =& v(t) + a(t) * \Delta t + \frac{1}{2} * b(t) * \Delta t^2 \\ x(t+\Delta t, p) =& x(t) + v(t) * \Delta t + \frac{1}{2} * a(t) * \Delta t^2 + \\ & \frac{1}{6} * b(t) * \Delta t^3 \end{aligned} \tag{17}$$

with the first and second derivative of the accelerations for GPC3 calculated as:

$$b(t) = \frac{\Delta a(t)}{\Delta t}, c(t) = 0 \tag{18}$$

In the evaluation step the difference in the accelerations calculated based on the acceleration $a(t+\Delta t, p)$ and the acceleration $a(t + \Delta t)$ calculated from positions $x(t+\Delta t, p)$ and velocities $v(t+\Delta t, p)$ is obtained by

$$\Delta a = a(t + \Delta t) - a(t + \Delta t, p) \tag{19}$$

In the following, correction step positions and their higher derivatives are calculated based on their values from the previous time step and the obtained difference in acceleration as

$$\begin{aligned} x(t+\Delta t) &= x(t+\Delta t, p) + k1 * \Delta a * \Delta t^2 \\ v(t+\Delta t) &= v(t+\Delta t, p) + k2 * \Delta a * \Delta t \\ a(t+\Delta t) &= a(t+\Delta t, p) + k3 * \Delta a \\ b(t+\Delta t) &= b(t+\Delta t, p) + k4 * \frac{\Delta a}{\Delta t} \end{aligned} \tag{20}$$

Gear's scheme parameters k1-k5 for GPC3: $k_1 = 1/12$, $k_2 = 5/12$, $k_3 = 1$, $k_4 = 1$, $k_5 = 0$

Numerical experiment

Comparing results

Discussion

References

[1] Matthew Danby, John Shrimpton, and Mark Palmer. "On the optimal numerical time integration for DEM using Hertzian force models". In: *Computers and Chemical Engineering* 58 (2013), pp. 211–222. ISSN: 00981354. DOI: 10.1016/j.compchemeng.2013.06.018.

[2] Vincent Iacobellis, Ali Radhi, and Kamran Behdinan. "Discrete element model for ZrB2-SiC ceramic composite sintering". In: *Composite Structures* 229 (2019), p. 111373. ISSN: 0263-8223. DOI: 10.1016/j.compstruct.2019.111373.

[3] Kevin J. Hanley and Catherine O'Sullivan. "Analytical study of the accuracy of discrete element simulations". In: *International Journal for Numerical Methods in Engineering* 109.1 (2017), pp. 29–51. ISSN: 10970207. DOI: 10.1002/nme.5275.

[4] Tyler Olsen and Ken Kamrin. "Resolving force indeterminacy in contact dynamics using compatibility conditions". In: *Granular Matter* 20.4 (2018), pp. 1–16. ISSN: 14347636. DOI: 10.1007/s10035-018-0839-5. URL: https://doi.org/10.1007/s10035-018-0839-5.

[5] V. Scherer et al. "Simulation of Reacting Moving Granular Material in Furnaces and Boilers An Overview on the Capabilities of the Discrete Element Method". In: *Energy Procedia* 120 (2017), pp. 41–61. ISSN: 18766102. DOI: 10.1016/j.egypro.2017.07.154. URL: http://dx.doi.org/10.1016/j.egypro.2017.07.154.

[6] Boxi Zhang et al. "Numerical investigation on the incipient motion of non-spherical sediment particles in bedload regime of open channel flows". In: *Computational Particle Mechanics* 7.5 (2020), pp. 987–1003. ISSN: 21964386. DOI: 10.1007/s40571-020-00323-8. URL: https://doi.org/10.1007/s40571-020-00323-8.

[7] Hrvoje Smoljanović et al. "Analysis of dynamic stability of beam structures". In: *Acta Mechanica* 231.11 (2020), pp. 4701–4715. ISSN: 16196937. DOI: 10.1007/s00707-020-02793-6.

[8] Mete Özgüz and M. Taner Eskil. "Numerical Integration Methods for Simulation of Mass-Spring-Damper Systems". In: *Computer and In-*

formation Sciences II. 2011. DOI: 10.1007/978-1-4471-2155-8_55.